Viral expression of insulin-like growth factor-I isoforms promotes different responses in skeletal muscle

Elisabeth R. Barton

Journal of Applied Physiology 100:1778-1784, 2006. First published Jan 26, 2006;
doi:10.1152/japplphysiol.01405.2005

Journal of Applied Physiology publishes original papers that deal with diverse areas of research in applied physiology, especially those papers emphasizing adaptive and integrative mechanisms. It is published 12 times a year (monthly) by the American Physiological Society, 9650 Rockville Pike, Bethesda MD 20814-3991. ISSN: 8750-7587, ESSN: 1522-1601. Visit our website at http://www.the-aps.org/.

J Appl Physiol 100: 1778–1784, 2006.
First published January 26, 2006; doi:10.1152/japplphysiol.01405.2005.

Viral expression of insulin-like growth factor-I isoforms promotes different responses in skeletal muscle

Elisabeth R. Barton

Department of Anatomy and Cell Biology, School of Dental Medicine, and Pennsylvania Muscle Institute, University of Pennsylvania, Philadelphia, Pennsylvania

Submitted 7 November 2005; accepted in final form 20 January 2006

Barton, Elisabeth R. Viral expression of insulin-like growth factor-I isoforms promotes different responses in skeletal muscle. *J Appl Physiol* 100: 1778–1784, 2006. First published January 26, 2006; doi:10.1152/japplphysiol.01405.2005.—Insulin-like growth factor I (IGF-I) is a critical protein for skeletal muscle development and regeneration. Its ability to promote skeletal muscle hypertrophy has been demonstrated by several methods. Alternative splicing of the *Igf-1* gene does not affect the mature IGF-I protein but does produce different E peptide extensions, which have been reported to modify the potency of IGF-I. Viral-mediated delivery of murine IGF-IA and IGF-IB into skeletal muscle of 2-wk-old and 6-mo-old mice was utilized to compare the effects of the isoforms on muscle mass. In young mice, tissue content of IGF-I protein was significantly higher in rAAV-treated muscles than control muscles at 1, 2, and 4 mo postinjection. Viral injection of IGF-IB produced two- to sevenfold more IGF-I than rAAVIGF-IA. Hypertrophy was observed 2 and 4 mo postinjection, where both rAAVIGF-IA and rAAVIGF-IB were equally effective in increasing muscle mass. These results suggest that there is a threshold of IGF-I production necessary to promote muscle hypertrophy in young growing animals regardless of isoform. In 6-mo-old animals, only rAAVIGF-IA produced significant increases in muscle size, even though increased IGF-I content was observed after injection of both isoforms. Therefore, the ability for IGF-IB to promote muscle hypertrophy is only effective in growing animals, suggesting that the bioavailability of this isoform or its receptor affinity diminishes with age.

adeno-associated virus; E peptide; IGF-I splicing

IT IS VIRTUALLY UNDISPUTED that increased insulin-like growth factor I (IGF-I) can promote increased muscle mass. Multiple methods have been utilized to demonstrate that IGF-I mediates skeletal muscle hypertrophy, including transgenic overexpression, viral-mediated delivery, directed infusion, and plasmid injection (2, 4, 9, 17, 21). Hypertrophy is produced both through ligand binding to IGF-I receptors (IGF-IR) on the skeletal muscle fibers and also through binding to receptors on activated satellite cells. The combined actions of these two mechanisms can drive protein synthesis and satellite cell proliferation and differentiation to provide a very effective increase in muscle size and strength.

Although there is general agreement that the IGF-I protein is one of the major mediators of these hypertrophic actions, there is a growing body of evidence that suggests that the isoform from which IGF-I is produced can affect its potency. Through multiple splicing at both the 5′ and 3′ ends of the gene, multiple classes, or isoforms, arise in mammals and fish (1, 8, 20). In rodents, there are four possible classes of IGF-I resulting from alternative splicing events, where class 1 and 2 denote the use of exon 1 or 2, respectively, and class A and B denote the absence or presence of exon 5 (Fig. 1*A*). All classes of prepropeptides produce an identical IGF-I protein. However, IGF-IB contains exon 5 of the *Igf-1* gene, which causes a frame shift and premature termination in exon 6 and results in a different E peptide extension (17, 20) in the IGF-I propeptide. IGF-IA is the predominant form expressed by muscle, liver, and several other tissues. The rodent IGF-IB is equivalent to human IGF-IC and has also been called mechano-growth factor (MGF) to indicate the increased expression of this isoform in response to stretch or damage (29, 30). Increased expression of human IGF-IC in response to eccentric contraction has been shown to diminish with age (18). MGF has been proposed to be a more potent form of IGF-I for promoting skeletal muscle hypertrophy after plasmid injection, to promote proliferation of muscle cells in culture, and to act through a novel receptor independent of the known IGF-I receptor (17, 31).

Early demonstration of mitogenic activity of one E peptide raised the possibility that the *Igf-1* gene produced two different bioactive factors (IGF-I and an E peptide), or, alternatively, the E peptide modified the actions of IGF-I. Exposure of cells to a peptide fragment within the human EB peptide (IBE1) resulted in increased mitogenic activity in bronchial epithelial cells (20). A later study utilized a different E-peptide fragment in human (which is also found in rodent IGF-IC/IGF-IB) and showed that cultures of C2C12 cells, an established muscle cell line, also increased proliferation in response to peptide exposure (24). The migration of the IGF-IB precursor differs from its more prevalent counterpart as well. Specifically, the inclusion of exon 5 leads to nucleolar localization, suggesting that IGF-I or the EB peptide had biological activity that did not involve the IGF-I receptors on the membrane (25).

To determine whether class 1 A and B IGF-I mediated different levels of skeletal muscle hypertrophy, viral-mediated gene transfer of each class was performed in young and adult mice. Young mice are assumed to have an active satellite pool as normal muscle growth progresses. In contrast, adult mice have ceased active growth, and so the satellite cell pool is dormant unless activated by damage. The use of two age groups provided the ability to distinguish the response of muscle to the IGF-I isoforms.

Address for reprint requests and other correspondence: E. R. Barton, Dept. of Anatomy and Cell Biology, 441A Levy Bldg., 240 S. 40th St., Univ. of Pennsylvania, Philadelphia, PA 19104 (e-mail: erbarton@biochem.dental.upenn.edu).

The costs of publication of this article were defrayed in part by the payment of page charges. The article must therefore be hereby marked "*advertisement*" in accordance with 18 U.S.C. Section 1734 solely to indicate this fact.

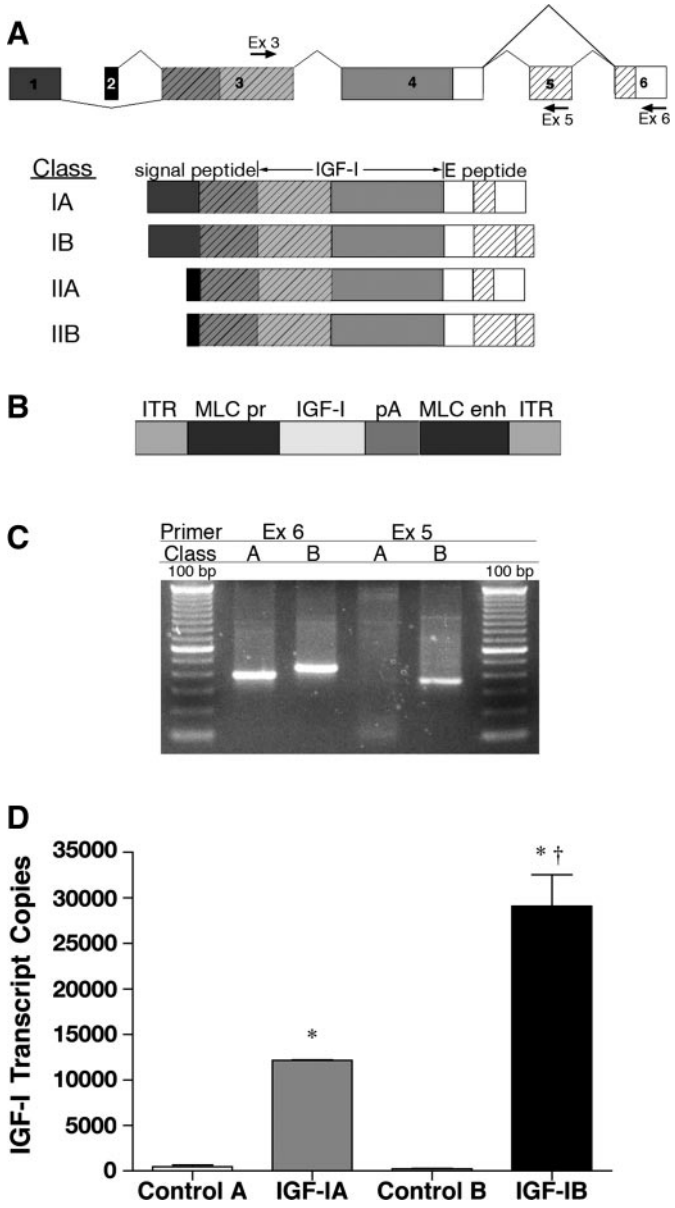

Fig. 1. IGF-I splice forms, viral construct, and expression analysis. *A*: the rodent Igf-1 gene contains 6 exons, in which exons 1 and 2 are alternatively utilized and comprise class I and II IGF-I, respectively. Exon 5 is normally absent (Class A), but when it is included (Class B) it causes a reading frame shift and premature stop in exon 6. Arrows indicate the sites of oligonucleotides for PCR (Ex 3, exon 3, sense; Ex 5, exon 5, antisense; Ex 6, exon 6, antisense). *B*: the cDNA encoding class I IGF-IA and IGF-IB was inserted into a transfer plasmid containing the MLC 1/3 promoter/enhancer (pr/enh) and an SV40 polyadenylation signal. The expression cassette was flanked by adeno-associated virus (AAV) inverted terminal repeats (ITR). *C*: PCR amplification of plasmids containing IGF-IA (*A*) and IGF-IB (*B*) with oligonucleotides shown in *A*. Ex 6 can detect both isoforms, whereas Ex 5 can detect only IGF-IB. *D*: real-time PCR for IGF-IA and IGF-IB expression at 1 mo after viral injection ($n = 3$ TA muscle pairs for each isoform). There was significantly more expression (*$P < 0.05$) of IGF-I in treated limbs compared with the contralateral control muscles. Injection of IGF-IB provided more expression than that of IGF-IA (†$P < 0.05$).

METHODS

Viral constructs. Murine class I *Igf-1A* and *Igf-1B* were amplified from RNA of neonatal murine skeletal muscle. Sequences were confirmed by comparisons to GenBank accession numbers AY878192 and AY878193, respectively, and contained the class I signal peptide, mature IGF-I, and the respective E peptide for each class (Fig. 1*A*). The open reading frames of each cDNA were inserted into the HindIII-SacI restriction sites in the pSUB201 vector containing the myosin light chain kinase 1/3 promoter/enhancer (12) (Fig. 1*B*). Recombinant adeno-associated virus serotype 2/8 (rAAV) was produced at the University of Pennsylvania Vector Core.

Injections. All experiments were approved by the university animal care committee. Animals were lightly anesthetized with ketamine-xylazine, and 1×10^{11} viral particles diluted in 75–100 μl of phosphate-buffered saline (PBS) were injected into the anterior compartment of one lower hindlimb of C57Bl/6 mice (male and female), targeting the tibialis anterior (TA) and extensor digitorum longus (EDL). The contralateral limb received an equal volume of PBS in the same manner as a control for the injection procedure. After injection, mice were allowed to recover from anesthesia and were housed in the animal facility until time of analysis. In one study, mice were 2–3 wk of age at the time of injection. Mice were killed at 1, 2, and 4 mo postinjection for analysis ($n = 4–8$ each time point and construct). In a second study, mice were injected at 6 mo of age and killed 4 mo postinjection for analysis ($n = 7$ each construct).

Functional analysis. Mice were anesthetized with ketamine-xylazine and exsanguinated. Blood samples were allowed to clot for 2 h at room temperature and then were centrifuged at 2,000 *g* for 20 min and then stored at −80°C for subsequent IGF-I content measurements. The TA and EDL muscles were removed and placed in a bath of Ringer solution gas equilibrated with 95% O_2-5% CO_2. The TA either was blotted, weighed, and rapidly frozen in liquid nitrogen for immunoblotting analysis or, after weighing, was homogenized in 1 ml of sterile PBS and frozen in liquid nitrogen for IGF-I content measurements. The EDL muscles were subjected to isolated muscle mechanical measurements by using a previously described apparatus (Aurora Scientific, Aurora, Ontario, Canada) (5). After determination of optimum length by single supramaximal twitch stimulation, maximum isometric tetanus was measured in the muscles from both limbs. On completion of mechanical measurements, EDL muscles were blotted, weighed, and rapidly frozen in melting isopentane.

Expression analysis. Muscles were removed from liquid nitrogen storage and ground with a mortar and pestle cooled with dry ice, and total RNA was isolated from the resultant powdered tissue (Trizol, Invitrogen, Carlsbad, CA). Quantification of RNA was performed with Ribogreen quantitation kit (Molecular Probes, Eugene, OR), and RNA integrity was confirmed by gel electrophoresis. Total RNA (150 ng) from each sample was subjected to single-strand reverse transcription (Applied Biosystems, Foster City, CA). The resultant cDNA was utilized for real-time PCR with oligonucleotides that were specific for IGF-IA and IGF-IB using the Roche Lightcycler system, and reagents (LightCycler FastStart DNA Master^{PLUS} SYBRgreen I). The location of these oligonucleotides within the IGF-I sequences and the resultant band size of the products are depicted in Fig. 1, *A* and *C*. The exon 6 oligonucleotide could detect both IGF-IA and IGF-IB, whereas the exon 5 oligonucleotide could only detect IGF-IB. Real-time PCR reactions contained 6 μl of cDNA, SYBRgreen master mix, 0.5 μM of each primer and nuclease free water to a total volume of 20 μl. IGF-I mRNA levels were assessed by calculating the crossing point (Cp), where measured fluorescence rises above background, as the second derivative maximum of the reaction curve. Each sample was analyzed in duplicate, and the resulting data were averaged. Quantification of expressed viral transgene copies was achieved by using plasmids containing the respective cDNAs. Serial dilutions of the plasmids provided the expected changes in Cp such that a 10-fold decrease in plasmid copy number resulted in a Cp that was approximately three cycles longer than the previous dilution. Melting-point analysis of control plasmids and experimental samples confirmed that the primers were specific for IGF-I, where there was only one melting point for each experimental sample that was not different from the

melting point with control plasmids. Controls included only RNA that was not subjected to reverse transcription and water.

Immunoblotting analysis. TA muscles were removed from liquid nitrogen storage and homogenized in 10 volumes/muscle wet weight of modified lysis buffer (50 mM Tris·HCl pH 7.4, 1% wt/vol Triton X-100, 0.25% sodium deoxycholate, 150 mM NaCl, 1 mM PMSF, 1 μg/ml aprotinin, 1 μg/ml leupeptin, 1 μg/ml pepstatin, 1 mM $NaVO_4$, 1 mM NaF, 1 mM EGTA). Homogenates were centrifuged to pellet debris, and the total protein was measured in the supernatant. Equal amounts of protein from each muscle lysate were separated by SDS-PAGE and transferred to polyvinylidene fluoride membranes (Immobilon-P, Millipore, Bedford, MA). Membranes were incubated in a blocking buffer [5% nonfat dry milk in Tris-buffered saline (TBS) plus 0.1% Tween 20 (5% milk-TTBS)] and then incubated in primary antibody diluted in 5% milk-TTBS overnight at 4°C. The following antibodies were used: phospho-Akt (no. 9271), total Akt (no. 9272), phospho-ERK1/2 (no. 9101), total ERK1/2 (no. 9102) (Cell Signaling, Beverly, MA). Membranes were then washed in 5% milk-TTBS and incubated with horseradish peroxidase-conjugated secondary antibody. After a series of washes in 5% milk-TTBS, TTBS, and TBS, protein detection was performed using enhanced chemiluminescence and the Kodak mm4000 detection system. Analysis of band intensity was performed by use of the associated image analysis software. Membranes were stained with Coomassie brilliant blue R-250 after immunoblotting to confirm equal protein loading.

Immunoprecipitation of IGF-I receptor complexes. Frozen TA muscles were ground and homogenized in buffer [100 mM HEPES (pH = 7.4); 150 mM NaCl; 5 mM EDTA; 5 mM $MgCl_2$; 2% NP-40; 1.5% Triton X-100, protease and phosphatase inhibitors (Sigma, St. Louis, MO)] and incubated at 4°C for 90 min with frequent vortexing. Samples were centrifuged at 10,000 *g* for 10 min at 4°C. Supernatants were transferred to new tubes and centrifuged at 150,000 *g* for 90 min at 4°C. The resultant supernatant was utilized for immunoprecipitation. A total of 500 μg of protein was incubated with protein A/G agarose (Santa Cruz Biotechnology, Santa Cruz, CA) for 30 min at 4°C. Samples were centrifuged for 2 min to collect the pellet, and the supernatant was exposed overnight to IGF-IR antibody (C-20, Santa Cruz Biotechnology) on a rocker at 4°C. Protein A/G agarose was then added for 6 h. The agarose pellet was collected by centrifugation and washed four times with PBS, then resuspended in 40 μl of 2× sample buffer, which was subjected to SDS-PAGE and subsequent immunoblotting (described in the previous section) with P-Tyr antibody (P-Tyr-100, no. 9411, Cell Signaling) to measure phosphorylated IGF-IR or IGF-IR antibody to measure total receptor.

Detection of IGF-I protein. The serum and TA homogenates were thawed, and the homogenates were centrifuged at 5,000 *g* for 5 min. The serum and supernatants were utilized for measurements of total IGF-I in a commercially available ELISA kit specific for rodent IGF-I (R&D Systems, Minneapolis, MN), and calculations of IGF-I content were based on a standard curve generated from recombinant mouse IGF-I. This kit detects total rodent IGF-I, and the measurements are not affected by the presence of IGF-I binding proteins or IGF-II. The assay can accurately detect IGF-I at 30–2,000 pg/ml with an intra-assay precision of 4.3% and an interassay precision of 5.9%. Preliminary experiments were performed on muscle samples from transgenic mice expressing rat IGF-IA under the MLC1/3 promoter/enhancer (21) to validate that the procedures used in the present study could accurately determine total IGF-I to the same degree as the acid-ethanol procedure used in a former study (3, 11). Preliminary experiments were also performed to verify that the TA and EDL from the same injection had similar IGF-I content. Measurements were acquired on a microtiter-plate reader (Dynatech Laboratories, Chantilly, VA) at 450 nm. All samples were measured in duplicate.

Statistics. Data are presented as means ± SE. Paired *t*-tests were utilized for comparisons between adeno-associated virus (AAV)-injected and contralateral control samples. One-way ANOVA was utilized for comparisons between IGF-I isoform treatments. Statistical significance was accepted for $P < 0.05$.

RESULTS

Expression of viral transgenes was assessed at 1 mo postinjection by real-time PCR ($n = 3$ muscle pairs for each IGF-I isoform). Both AAV constructs provided strong expression of the IGF-I isoforms above the endogenous expression level (Fig. 1*D*). rAAVIGF-IB produced significantly more expression than rAAVIGF-IA. To ensure that the increased expression was specific for the isoform that had been injected, both primer pairs were utilized for all muscles. These measurements confirmed that rAAVIGF-IA produced only IGF-IA transcripts and that rAAVIGF-IB produced only IGF-IB transcripts (data not shown).

IGF-I can activate both the PI3K/Akt pathway and the MAPK pathways via IGF-I receptor binding and activation (6, 10, 23). To test for differences in activation of these pathways by the IGF-I isoforms, immunoblotting was performed on muscle homogenates 1 mo postinjection ($n = 3$ muscle pairs for each IGF-I isoform). Both IGF-I isoforms produced robust IGF-IR and Akt phosphorylation compared with sham-injected control limbs (Fig. 2). Injection of rAAVIGF-IB also resulted in an increase of phosphorylated ERK1/2, which was not evident in rAAVIGF-IA-injected muscles and also produced more phosphorylation of IGF-IR than IGF-IA. There was no change in the content of IGF-IR, Akt, or ERK1/2 in rAAV-injected limbs compared with sham-injected limbs.

Muscle IGF-I content as measured by ELISA increased significantly by the injection of either isoform at 1 mo postinjection and remained higher than the control limbs for the

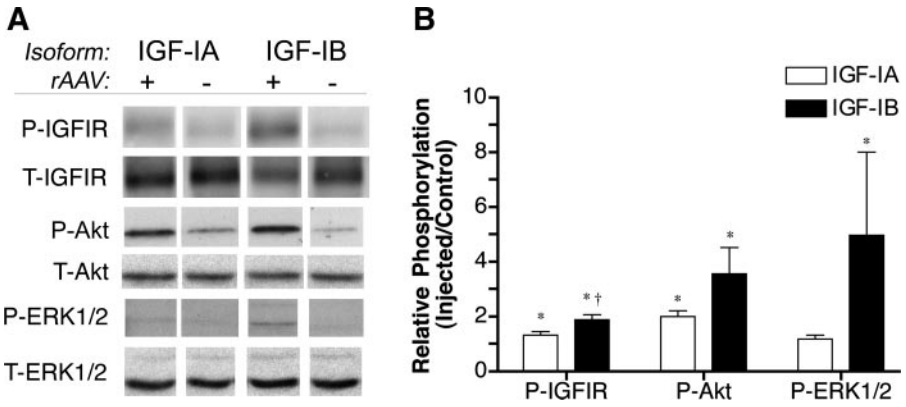

Fig. 2. Immunoblot (*A*) and analysis (*B*) of tibialis anterior (TA) muscles treated with recombinant adeno-associated virus (rAAV) expressing each IGF-I isoform 4 wk postinjection ($n = 3$ muscle pairs for each isoform). Skeletal muscle exhibited increased phosphorylated IGF-IR and Akt (P-IGFIR, P-Akt) in response to both isoforms. Only rAAVIGF-IB evoked changes in phosphorylated ERK1/2 (P-ERK1/2) in treated muscles and showed significantly more P-IGF-IR. Injection of PBS did not affect P-Akt or P-ERK1/2 (rAAV minus columns). Total IGF-IR, Akt, and ERK1/2 (T-IGFIR, T-Akt, T-ERK1/2) did not differ between limbs. *$P = 0.05$ for comparisons between treated and untreated limbs; †$P < 0.05$ for comparisons between isoforms.

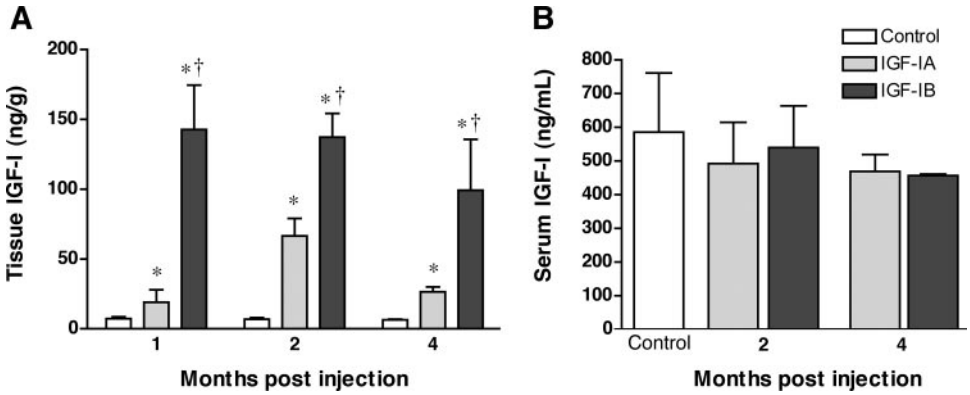

Fig. 3. Effect of viral delivery on IGF-I protein in young animals. *A*: tissue levels of IGF-I in tibialis anterior muscles were significantly increased by viral delivery of both IGF-IA and IGF-IB at 1 ($n = 3$ for each isoform), 2 ($n = 3$ for each isoform), and 4 ($n = 6$ for each isoform) mo postinjection compared with sham-injected contralateral muscles. Injection of the rAAVIGF-IB produced 2- to 7-fold more IGF-I than did rAAVIGF-IA. *B*: serum levels of total IGF-I in rAAV-injected animals at 2 ($n = 6$ for each isoform) and 4 ($n = 3$ for each isoform) mo postinjection were not different from levels measured in untreated 10-wk-old mice ($n = 3$). *$P < 0.05$ for paired comparisons of AAV-injected and control muscles (Student's *t*-test); †$P < 0.05$ for comparisons between groups (1-way ANOVA).

duration of the study (Fig. 3*A*). The levels of IGF-I protein produced exceeded that produced by transgenic expression of rat IGF-IA under the same promoter (3). Interestingly, rAAVIGF-IB generated much higher levels of IGF-I protein than rAAVIGF-IA at all time points. Total IGF-I in rAAVIGF-IB-injected muscles achieved levels as high as 231 ng/g tissue. Serum IGF-I was also monitored to determine whether increased tissue content of IGF-I resulted in changes in content of IGF-I in the circulation. There was no significant change in serum IGF-I regardless of isoform at 2 and 4 mo postinjection of rAAV compared with serum from 10-wk-old untreated mice (Fig. 3*B*).

The mass of EDL muscles was determined at 1, 2, and 4 mo post-rAAV injection in young animals ($n = 4–8$ animals per construct and time point) (Fig. 4*A*). At 1 mo, there was no significant difference in muscle mass between treated and control EDL muscles. By 2 mo, hypertrophy was observed in EDL muscles treated with either IGF-I isoform compared with the contralateral control muscles, where there was a 12 ± 2 and $7 \pm 2\%$ increase in mass for rAAVIGF-IA- and rAAVIGF-IB-injected EDLs, respectively ($n = 7$ for each virus). Hypertrophy was maintained to 4 mo. There was no difference in the increases in muscle mass achieved by either IGF-I isoform, even though there was more total IGF-I produced by IGF-IB AAV (Fig. 3*A*). Although not directly tested in this study, it appeared that there was a threshold of IGF-I protein that had to be reached to promote hypertrophy, and levels of IGF-I above that did not produce more muscle mass. Because the functional and morphological changes increased proportionally, there was no significant difference in specific force of isolated EDL muscles between treatments (Fig. 4*B*).

To address whether there was an effect of growth on IGF-I isoform-mediated hypertrophy, mice were injected with rAAV at 6 mo of age and analyzed 4 mo postinjection ($n = 7$ animals per construct). Both rAAV constructs produced increased IGF-I protein, and, similar to young animals, the rAAVIGF-IB had significantly higher production of IGF-I than that of rAAVIGF-IA (Fig. 5*A*). The total levels of IGF-I appeared lower than that observed in younger animals but were not significantly different (by one-way ANOVA) (Fig. 3*A*). There was no difference in serum IGF-I in animals injected with either construct, nor were the serum levels different from those

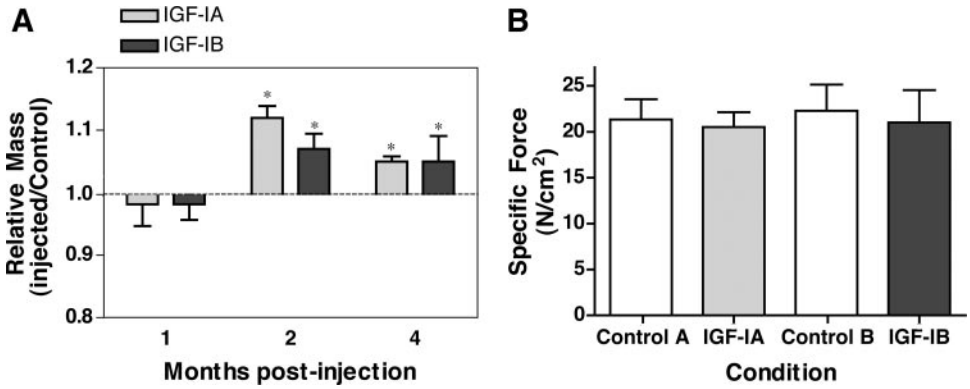

Fig. 4. Effect of viral IGF-I delivery on muscle mass and function in young animals. *A*: relative muscle mass was not affected by increased IGF-I protein at 1 mo postinjection ($n = 4$ for each isoform). By 2 mo ($n = 5$ for each isoform), both constructs produced hypertrophy in the treated extensor digitorum longus (EDL) muscles, and the effect was maintained until 4 mo postinjection ($n = 5$ muscle pairs for IGF-IA, $n = 6$ for IGF-IB). There was no difference between the two isoforms in the amount of hypertrophy produced. *B*: specific force in EDL muscles at 4 mo postinjection was not different than contralateral controls, which indicated that the increased muscle mass produced comparable increased tetanic force; $n = 5$ muscle pairs for IGF-IA, $n = 6$ for IGF-IB for functional analysis. *$P < 0.05$ for paired comparisons of AAV-injected and control muscles (Student's *t*-test).

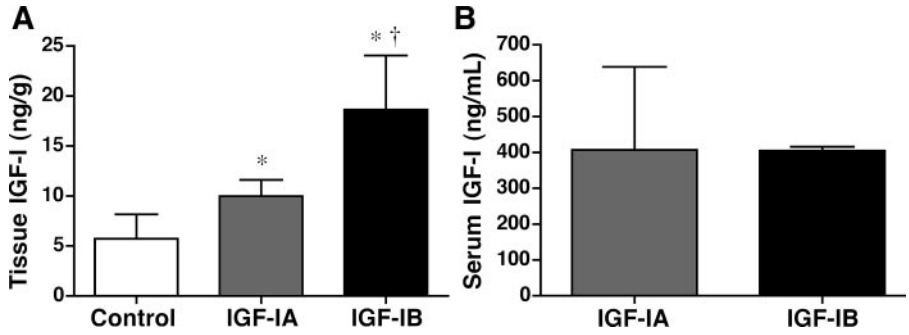

Fig. 5. Effect of viral delivery on IGF-I protein in mature 6-mo-old animals. *A*: tissue levels of total IGF-I doubled in rAAVIGF-IA TA muscles ($n = 4$) and were 4-fold higher in rAAVIGF-IB TA muscles ($n = 5$) compared with contralateral controls. *B*: there was no difference in serum levels of total IGF-I between animals treated with either rAAV at 4 mo postinjection ($n = 3$ for each isoform). *$P <$ 0.05 for paired comparisons of AAV-injected and control muscles (Student's *t*-test); †$P < 0.05$ for comparisons between groups (1-way ANOVA).

from younger animals (Fig. 5*B*). Mass and function were also determined in muscles from older mice that had been injected with AAV at 6 mo of age (Fig. 6*A*). At 4 mo postinjection, there was ~5% increase in muscle mass only in IGF-IA AAV-injected muscles, whereas no difference could be detected in IGF-IB AAV-injected muscles compared with contralateral control limbs. Tetanic force increased in concert with hypertrophy, and, as in young muscles, specific force was not changed due to injection of either isoform (Fig. 6*B*). Comparisons between young and mature animals at 4 mo postinjection showed that there were no statistical differences in mass increases.

DISCUSSION

This study tested whether increased expression of class I A and B IGF-I affected skeletal muscle mass differently. The results show that there are several distinguishing features of these isoforms. First, even though both isoforms cause increased phosphorylation of the IGF-IR, increased expression of IGF-IB drives both the PI-3K/Akt pathway and the MAPK pathway as monitored by increased P-Akt and P-ERK1/2, whereas IGF-IA expression results in increased P-Akt only. Viral-mediated delivery of each construct causes increased IGF-I expression and total IGF-I content in muscle as early as 1 mo postinjection, and IGF-IB produces significantly more IGF-I transcription and protein than IGF-IA. Total IGF-I in the serum was not affected by either construct with single-limb injections. Resultant hypertrophy by these constructs did not differ in young growing animals; however, in skeletally mature adult animals, only IGF-IA promoted significant increases in muscle mass. These results suggest that IGF-IB might be able to accumulate more efficiently in young muscle tissue, but that it is not more potent than IGF-IA in promoting hypertrophy. In fact, this class is ineffective in driving muscle hypertrophy in mature animals.

The recent discovery of new AAV serotypes has improved the ability for viral-mediated gene delivery to efficiently transduce target tissues. AAV serotype 8 (AAV-2 genomes pseudopackaged into AAV-8 capsids) has very high tropism for skeletal muscle and an accelerated time course for gene expression (15, 26). As shown in Figs. 1*D* and 2*A*, high levels of IGF-I RNA and protein are present as early as 1 mo postinjection, which is more rapid than that achieved in former studies of IGF-I-mediated hypertrophy with different serotypes (4, 19). The deletion of the 5′ untranslated region (UTR) in the constructs utilized in this study could also contribute to increased total IGF-I. Viral expression of class A and B IGF-I exceeded levels obtained by transgenic expression with the same promoter (3, 21) and approached those obtained by transgenic expression of human IGF-IA lacking the 5′ UTR (9). The 5′ UTR harbors multiple AUG translation initiation codons followed by in-frame termination codons that can impair the ability to initiate protein synthesis at the correct authentic start site (13, 14, 27). Therefore, the removal of these regulatory regions from the open reading frame of *Igf-1* gene improved production of IGF-I from a strong skeletal muscle-specific promoter.

Even with these modifications, it is surprising that that rAAVIGF-IB produced significantly more IGF-I mRNA and protein than rAAVIGF-IA. Identical numbers of viral particles were introduced for each construct, so the difference cannot be explained by differences in viral titer. The sole difference between the construct is the inclusion of exon 5 in rAAVIGF-IB. In light of the lower endogenous expression of IGF-IB that has been observed in other studies (18), it is possible that there is enhanced transcription and translation of the *Igf-1B* that

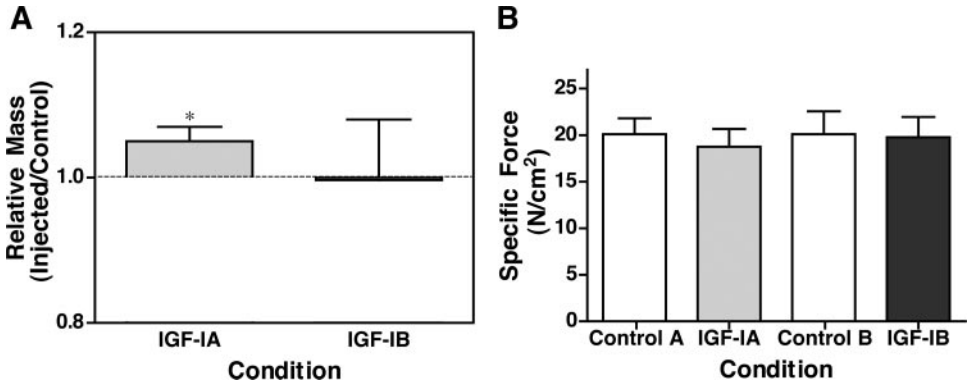

Fig. 6. Effect of viral delivery on muscle mass and function in 6-mo-old animals. *A*: EDL muscle mass increased 5% with rAAVIGF-IA 4 mo postinjection, whereas no hypertrophy was observed in those treated with rAAVIGF-IB. *B*: specific force was not significantly different in the EDL muscles from experimental or control groups; $n = 7$ muscle pairs for each isoform. *$P < 0.05$ for paired comparisons of AAV-injected and control muscles (Student's *t*-test).

results in greater accumulation of IGF-I protein. This issue was not resolved in these experiments, and the effect that the E peptide has on the efficiency of transcription or translation will require testing in future studies.

The signaling pattern also differs between the two IGF-I isoforms. As former studies in vitro and in vivo have established, the PI-3K/Akt pathway has been linked predominantly to myogenic actions and the hypertrophic responses to IGF-I, whereas both the PI-3K/Akt and MAPK pathways have been implicated in mitogenic actions of IGF-I (6, 7, 10, 22, 23). The fact that only IGF-IB caused increased P-ERK1/2 was consistent with previous observations that the EB peptide promoted cell proliferation (24, 31). However, at the 1-mo time point in the study, rAAVIGF-IB produced approximately seven times more IGF-I than rAAVIGF-IA, and so it is not clear whether ERK1/2 phosphorylation is the result of differences in isoform specification to signal transduction pathways or merely that the increased level of IGF-I production by AAVIGF-IB reveals the dose-response sensitivity of these signaling pathways.

It is intriguing that, even with higher production of total IGF-I by rAAVIGF-IB, the level of hypertrophy achieved in young growing animals by either construct was indistinguishable. In both cases, the IGF-I levels must have been above the necessary threshold for hypertrophy to occur. Alternatively, the bioavailability of IGF-I could have been restricted by increased expression of binding proteins. Only total IGF-I was measured, and so it is not known how much free IGF-I was available to bind to IGF-I receptors. Whether IGF-IB affects binding protein expression or has greater affinity for existing binding proteins in the muscle matrix has yet to be determined but will be important to clarify in future studies.

The effects of rAAVIGF-IA in mature animals, where a 5% increase in mass was achieved, are reminiscent of the amount of hypertrophy achieved after gamma radiation (5). The presence of viral IGF-I in irradiated muscle produced a 5% increase in muscle mass compared with irradiation alone. In both cases, the satellite cell pool is quiescent, either by inhibition of proliferation by irradiation in the former study, or because there is little active growth in 6-mo-old animals utilized in the present study. The ability for rAAVIGF-IA to promote modest hypertrophy in the absence of an active satellite cell pool suggests that this isoform can bind to and activate IGF-I receptors on the muscle fibers.

Although the serotype and exact sequence injected differs between the present and former studies (4, 5, 19), the increased IGF-IA expression promoted equivalent levels of hypertrophy in young growing animals. However, the effect of IGF-IA in mature animals may be quite different than that observed in aging animals. As described above, increased IGF-IA could promote modest hypertrophy in mature animals, whereas muscle mass was maintained and not increased as the animals aged from 18 to 27 mo (4). Whether the 18-mo-old animals exhibited hypertrophy to the same extent as 6-mo-old animals at 4 mo postinjection or whether by 27 mo of age the 6-mo-old treated animals still exhibit hypertrophy has not been addressed. These comparisons will help to clarify the importance of an activated satellite cell pool vs. muscle fiber receptor activation in promotion of muscle hypertrophy and maintenance of muscle mass.

In contrast, the introduction of rAAVIGF-IB did not affect muscle mass at all in mature animals, even though there was more total IGF-I present. In addition, unlike plasmid delivery of IGF-IB (MGF) to young animals in which hypertrophy was observed 2 wk postinjection (16), viral delivery of IGF-IB did not promote hypertrophy until 2 mo after injection. Again, these differences might be explained by the presence of an activated satellite cell population subjected to IGF-IB. Plasmid delivery provides rapid, although inefficient expression, such that transgene expression is concurrent with the damage inevitably caused by the injection itself and with satellite cells that have been activated to repair the muscle tissue (28). If the target for IGF-IB is an activated satellite cell, there is a pool of them surrounding the injection site for the IGF-IB plasmid. Unlike plasmid DNA, rAAV DNA is single stranded and requires complementation before expression, therefore delaying expression until ~2 wk postinjection. At this point, the muscle repair process is well underway, and the pool of activated satellite cells is reduced as they fuse to muscle fibers. The temporal separation between damage due to injection and expression of IGF-IB limits the population of activated satellite cells to those involved in normal growth.

These results suggest three possibilities. First, more of the IGF-I produced by rAAVIGF-IB could be bound to IGF-I binding proteins and is therefore unavailable for activating the IGF-I receptors on the muscle fibers. Second, the IGF-I receptors on the muscle fibers might have a lower affinity for IGF-I produced by rAAVIGF-IB. Third, IGF-I produced by rAAVIGF-IB might only bind to receptors on activated satellite cells. Because the IGF-I protein produced by any isoform is identical, these potential mechanisms would require that the remaining E peptide extension be involved in dictating the responses observed in this study. The generation of constructs harboring only the E peptide without the sequence encoding IGF-I as well as constructs lacking the sequence for the E peptide will be required to test how important the E peptide extensions are for IGF-I effects in skeletal muscle.

Previous studies have identified the EB peptide as a key effector of the mitogenic actions of IGF-I. The results described here are, in part, consistent with this hypothesis, for the proliferative effects in skeletal muscle rely on activated satellite cells. When there is an active satellite cell pool, such as in young growing muscle, IGF-IB can promote hypertrophy to an extent similar to that achieved by IGF-IA. When active satellite cells are diminished, such as in the 6-mo-old animals, IGF-IB cannot promote hypertrophy. Alternative proposals have suggested the presence of a novel receptor to which only IGF-IB can bind (24, 31). Although the present study cannot rule out this possibility, it is clear that both isoforms can activate the IGF-IR. However, the parameters tested here indicate that the proposed novel receptor must only be available in young growing animals, and so identification might be achieved in comparisons of receptor populations of young and old muscle.

In summary, a comparison of the effects of class I IGF-IA and IGF-IB in skeletal muscle reveal that the isoforms are not identical. Production of IGF-I is achieved more efficiently by IGF-IB. However, the ability of this isoform to promote muscle hypertrophy is not greater than IGF-IA in young growing muscle, and it is virtually nonexistent in adult muscle. These observations are counter to the implication that this isoform is a more potent form of IGF-I, yet there are clear differences in the accumulation and bioavailability between the classes of IGF-I, which should be explored further.

ACKNOWLEDGMENTS

Viral production was performed at the University of Pennsylvania Vector Core. E. R. Barton is grateful to Jessie Feng, Rong-Ine Ma, and Kevin Morine for technical support.

GRANTS

Support for this study was from the University Research Foundation, a Rabinowitz Award for Excellence in Research, and National Institute of Arthritis and Musculoskeletal and Skin Diseases Grant AR-050160.

REFERENCES

1. **Adamo ML, Neuenschwander S, LeRoith D, and Roberts CT Jr.** Structure, expression, and regulation of the IGF-1 gene. *Adv Exp Med Biol* 343: 1–11, 1993.
2. **Adams GR and McCue SA.** Localized infusion of IGF-I results in skeletal muscle hypertrophy in rats. *J Appl Physiol* 84: 1716–1722, 1998.
3. **Barton ER, Morris L, Musaro A, Rosenthal N, and Sweeney HL.** Muscle-specific expression of insulin-like growth factor I counters muscle decline in mdx mice. *J Cell Biol* 157: 137–148, 2002.
4. **Barton-Davis ER, Shoturma DI, Musaro A, Rosenthal N, and Sweeney HL.** Viral mediated expression of insulin-like growth factor I blocks the aging-related loss of skeletal muscle function. *Proc Natl Acad Sci USA* 95: 15603–15607, 1998.
5. **Barton ER.** Impact of sarcoglycan complex on mechanical signal transduction in murine skeletal muscle. *Am J Physiol Cell Physiol* 290: C411–C419, 2006.

5a. **Barton-Davis ER, Shoturma DI, and Sweeney HL.** Contribution of satellite cells to IGF-I induced hypertrophy of skeletal muscle. *Acta Physiol Scand* 167: 301–305, 1999.

6. **Bodine SC, Stitt TN, Gonzalez M, Kline WO, Stover GL, Bauerlein R, Zlotchenko E, Scrimgeour A, Lawrence JC, Glass DJ, and Yancopoulos GD.** Akt/mTOR pathway is a crucial regulator of skeletal muscle hypertrophy and can prevent muscle atrophy in vivo. *Nat Cell Biol* 3: 1014–1019, 2001.
7. **Chakravarthy MV, Abraha TW, Schwartz RJ, Fiorotto ML, and Booth FW.** Insulin-like growth factor-I extends in vitro replicative life span of skeletal muscle satellite cells by enhancing G1/S cell cycle progression via the activation of phosphatidylinositol 3′-kinase/Akt signaling pathway. *J Biol Chem* 275: 35942–35952, 2000.
8. **Chen MH, Lin G, Gong H, Weng C, Chang C, and Wu J.** The characterization of prepro-insulin-like growth factor-1 Ea-2 expression and insulin-like growth factor-1 genes (devoid 81 bp) in the zebrafish (*Danio rerio*). *Gene* 268: 67–75, 2001.
9. **Coleman ME, DeMayo F, Yin KC, Lee HM, Geske R, Montgomery C, and Schwartz RJ.** Myogenic vector expression of insulin-like growth factor I stimulates muscle cell differentiation and myofiber hypertrophy in transgenic mice. *J Biol Chem* 270: 12109–12116, 1995.
10. **Coolican SA, Samuel DS, Ewton DZ, McWade FJ, and Florini JR.** The mitogenic and myogenic actions of insulin-like growth factors utilize distinct signaling pathways. *J Biol Chem* 272: 6653–6662, 1997.
11. **D'Ercole AJ, Stiles AD, and Underwood LE.** Tissue concentrations of somatomedin C: further evidence for multiple sites of synthesis and paracrine or autocrine mechanisms of action. *Proc Natl Acad Sci USA* 81: 935–939, 1984.
12. **Donoghue M, Ernst H, Wentworth B, Nadal-Ginard B, and Rosenthal N.** A muscle-specific enhancer is located at the 3′ end of the myosin light-chain 1/3 gene locus. *Genes Dev* 2: 1779–1790, 1988.
13. **Foyt HL, Lanau F, Woloschak M, LeRoith D, and Roberts CT Jr.** Effect of growth hormone on levels of differentially processed insulin-like growth factor I mRNAs in total and polysomal mRNA populations. *Mol Endocrinol* 6: 1881–1888, 1992.
14. **Foyt HL, LeRoith D, and Roberts CT Jr.** Differential association of insulin-like growth factor I mRNA variants with polysomes in vivo. *J Biol Chem* 266: 7300–7305, 1991.
15. **Gao GP, Alvira MR, Wang L, Calcedo R, Johnston J, and Wilson JM.** Novel adeno-associated viruses from rhesus monkeys as vectors for human gene therapy. *Proc Natl Acad Sci USA* 99: 11854–11859, 2002.
16. **Goldspink G.** Cloning of local growth factors involved in the determination of muscle mass. *Br J Sports Med* 34: 159–160, 2000.
17. **Goldspink G.** Mechanical signals, IGF-I gene splicing, and muscle adaptation. *Physiology (Bethesda)* 20: 232–238, 2005.
18. **Hameed M, Orrell RW, Cobbold M, Goldspink G, and Harridge SD.** Expression of IGF-I splice variants in young and old human skeletal muscle after high resistance exercise. *J Physiol* 547: 247–254, 2003.
19. **Lee S, Barton ER, Sweeney HL, and Farrar RP.** Viral expression of insulin-like growth factor-I enhances muscle hypertrophy in resistance-trained rats. *J Appl Physiol* 96: 1097–1104, 2004.
20. **Lund PK.** Insulin-like growth factors: gene structure and regulation. In: *Handbook of Physiology. The Endocrine System. Cellular Endocrinology*. Bethesda, MD: Am. Physiol. Soc., 1998, sect. 7, pt. I, p. 537–571.
21. **Musaro A, McCullagh K, Paul A, Houghton L, Dobrowolny G, Molinaro M, Barton ER, Sweeney HL, and Rosenthal N.** Localized Igf-1 transgene expression sustains hypertrophy and regeneration in senescent skeletal muscle. *Nat Genet* 27: 195–200, 2001.
22. **Petley T, Graff K, Jiang W, Yang H, and Florini J.** Variation among cell types in the signaling pathways by which IGF-I stimulates specific cellular responses. *Horm Metab Res* 31: 70–76, 1999.
23. **Rommel C, Bodine SC, Clarke BA, Rossman R, Nunez L, Stitt TN, Yancopoulos GD, and Glass DJ.** Mediation of IGF-1-induced skeletal myotube hypertrophy by PI(3)K/Akt/mTOR and PI(3)K/Akt/GSK3 pathways. *Nat Cell Biol* 3: 1009–1013, 2001.
24. **Siegfried JM, Kasprzyk PG, Treston AM, Mulshine JL, Quinn KA, and Cuttitta F.** A mitogenic peptide amide encoded within the E peptide domain of the insulin-like growth factor IB prohormone. *Proc Natl Acad Sci USA* 89: 8107–8111, 1992.
25. **Tan DS, Cook A, and Chew SL.** Nucleolar localization of an isoform of the IGF-I precursor. *BMC Cell Biol* 3: 17, 2002.
26. **Wang Z, Zhu T, Qiao C, Zhou L, Wang B, Zhang J, Chen C, Li J, and Xiao X.** Adeno-associated virus serotype 8 efficiently delivers genes to muscle and heart. *Nat Biotechnol* 23: 321–328, 2005.
27. **Willis AE.** Translational control of growth factor and proto-oncogene expression. *Int J Biochem Cell Biol* 31: 73–86, 1999.
28. **Wolff JA and Budker V.** The mechanism of naked DNA uptake and expression. *Adv Genet* 54: 3–20, 2005.
29. **Yang H, Alnaqeeb M, Simpson H, and Goldspink G.** Changes in muscle fibre type, muscle mass and IGF-I gene expression in rabbit skeletal muscle subjected to stretch. *J Anat* 190: 613–622, 1997.
30. **Yang S, Alnaqeeb M, Simpson H, and Goldspink G.** Cloning and characterization of an IGF-1 isoform expressed in skeletal muscle subjected to stretch. *J Muscle Res Cell Motil* 17: 487–495, 1996.
31. **Yang SY and Goldspink G.** Different roles of the IGF-I Ec peptide (MGF) and mature IGF-I in myoblast proliferation and differentiation. *FEBS Lett* 522: 156–160, 2002.